

Viscosity of Water + *tert*-Butyl Alcohol (2-Methyl-2-propanol) Mixtures at Low Temperatures and High Pressure[†]

Kenneth R. Harris* and Lawrence A. Woolf

School of Physical, Environmental, and Mathematical Sciences, University College, University of New South Wales, Australian Defence Force Academy, Canberra, ACT 2600, Australia

The viscosity of dilute aqueous solutions of 2-methyl-2-propanol (*tert*-butyl alcohol, TBA) has been measured between (−10 and 25) °C with a falling-body viscometer to a maximum pressure of 388 MPa. The expanded uncertainty is estimated at ± 2 %. Comparison is made with earlier measurements of the intradiffusion coefficient of water in TBA solutions under similar conditions. (K. R. Harris and P. J. Newitt, *J. Phys. Chem. A* **1999**, *103*, 6508). At the higher concentrations, the fluidity, like the water self-diffusion coefficient, is linear in the solution molar volume. As the solutions become more dilute and the molar volume decreases, fluidity maxima appear, first at the lower temperatures, then gradually extending to higher temperatures. The positions of the maxima vary with composition and temperature. Relative to the values at atmospheric pressure, the maxima in the more dilute solutions ($x = 0.01, 0.025$) are greater than those for pure water under the same conditions and shifted to slightly higher pressures. Consistent with conclusions drawn from high-pressure neutron-scattering studies (V. Calandrini et al. *J. Phys.: Condens. Matter* **2006**, *18*, S2363), it appears that the effect of the dissolved solute is similar to that of a temperature drop of 5 K in pure water in terms of the effect on the relative viscosity.

Introduction

Alcohol–water mixtures are an important class of solvents that have attracted a great deal of experimental, computational, and theoretical investigation. For example, they have been used as solvent systems for studies of the electrical conductivity of strong and weak electrolytes. Varying the composition changes the viscosity and the dielectric constant, and both these quantities appear in the models used to describe the ion–ion interactions in such systems.^{1–4} Studies of the hydrophobic effect have been another major application, the aim being to examine how, and even whether, water structure is affected by a nonpolar group in a small molecule readily solvated by water and how this information might be applied to understand the forces that control the structure of biomolecules in aqueous solution.^{5–7}

Of the small alcohols fully miscible with water near room temperature and atmospheric pressure, 2-methyl-2-propanol (*tert*-butanol or TBA) has been regarded as the most “hydrophobic” due to the symmetry and compactness of its alkyl group. Extensive neutron scattering studies have been made in recent years of the solution structure by Finney, Soper, Bowron, and co-workers, principally at low concentrations in the mole fraction range 0.02 to 0.16.^{8–12} They have concluded that structural changes are produced in the second hydration sphere of a water molecule,^{7,9} rather than the first, and that there are no clathrate-like first hydration structures or classical Frank–Wen “icebergs” around solute molecules in dilute solutions. Rather, at TBA mole fractions $x = 0.02$ and 0.04 , the TBA molecules tend to cluster with direct nonpolar headgroup contacts.^{9,10} Hydrogen–deuterium isotopic substitution techniques have been employed, so that any isotope effects in solution structure are necessarily smoothed out, and the solution

Table 1. Density ρ of Aqueous TBA Solutions

x $\theta/^\circ\text{C}$	0.00982	0.02462	0.05982	0.09495
	$\rho/\text{g}\cdot\text{cm}^{-3}$			
0.00	0.993577	0.987471	0.979211	0.963617
10.00	0.993663	0.987187	0.976858	0.959886
20.00	0.992714	0.985566	0.971477	0.952493
25.00	0.990540	0.982769	0.965475	0.945112

Table 2. Tait Equation Parameters, $\rho = \rho(0.1 \text{ MPa})/(1 - C \ln [(B + p)/(B + 0.1)])$

x	$\theta/^\circ\text{C}$	25	15	5	0	−5	−10
0 ^a	B/MPa	286.5	268.9	247.4	235.6		
	C	0.1318	0.1286	0.1251	0.1237		
0.00982	B/MPa	337.7	313.6	288.9	269.8	249.1	
	C	0.1463	0.1385	0.1380	0.1388	0.1384	
0.02462	B/MPa	330.9	344.7	334.6	340.4	339.8	
	C	0.1460	0.1433	0.1479	0.1499	0.1517	
0.05982	B/MPa	285.6	305.6	384.3	394.5	416.8	440.4
	C	0.1138	0.1278	0.1376	0.1497	0.1564	0.1639
0.09495	B/MPa	209.1	214.6	220.3	223.9		
	C	0.1034	0.1022	0.1031	0.1031		

^a Derived from data calculated from NIST/ASME (IAPWS 1995) Steam Database ver. 2.2 for pure water.

structure is determined as the result of iterative Monte-Carlo computations used to best fit the experimental scattering data. These studies have been conducted near and above room temperature, as the hydrophobic effect increases with temperature.¹³ To cite Southall, Dill and Haymet,¹⁴ “Hydrophobicity is entropic in cold water, and enthalpic in hot water”. On the other hand, the anomalous behavior of water, relative to other molecular liquids, and of its solutions is more pronounced at subambient temperatures.¹⁵

This laboratory has previously reported high-pressure studies of the intradiffusion coefficient of water in dilute TBA solutions in the range (−10 to 25) °C at pressures to approximately 400

* To whom correspondence should be addressed. E-mail: k.harris@adfa.edu.au.

[†] Part of the special issue “Robin H. Stokes Festschrift”.

Table 3. Viscosity η of Aqueous TBA Solutions

$x = 0.00982, \theta = 25.00\text{ }^{\circ}\text{C}$				$x = 0.00982, \theta = 25.00\text{ }^{\circ}\text{C}$				$x = 0.02462, \theta = 25.00\text{ }^{\circ}\text{C}$				$x = 0.02462, \theta = 25.00\text{ }^{\circ}\text{C}$			
p/MPa	t/s	$\rho/\text{g}\cdot\text{cm}^{-3}$	$\eta/\text{mPa}\cdot\text{s}$	p/MPa	t/s	$\rho/\text{g}\cdot\text{cm}^{-3}$	$\eta/\text{mPa}\cdot\text{s}$	p/MPa	t/s	$\rho/\text{g}\cdot\text{cm}^{-3}$	$\eta/\text{mPa}\cdot\text{s}$	p/MPa	t/s	$\rho/\text{g}\cdot\text{cm}^{-3}$	$\eta/\text{mPa}\cdot\text{s}$
0.1	36.10	0.99054	1.087	175.5	37.35	1.05510	1.114	0.1	48.21	0.98277	1.453	150.5	50.29	1.03962	1.504
0.1	36.16	0.99054	1.089	200.5	37.81	1.06298	1.126	0.3	48.12	0.98284	1.451	174.9	50.83	1.04762	1.518
0.4	36.09	0.99065	1.087	225.5	38.27	1.07060	1.139	1.2	48.05	0.98326	1.449	199.7	51.54	1.05549	1.537
6.2	36.08	0.99313	1.086	250.5	38.84	1.07802	1.155	3.0	48.14	0.98401	1.451	224.4	52.29	1.06306	1.558
11.3	36.07	0.99530	1.085	275.5	39.41	1.08520	1.170	5.5	48.18	0.98509	1.452	250.2	53.10	1.07076	1.580
25.7	36.02	1.00124	1.083	300.5	40.03	1.09220	1.187	10.6	48.18	0.98726	1.452	275.1	53.80	1.07794	1.599
50.2	36.04	1.01098	1.082	325.5	40.66	1.09900	1.205	25.2	48.29	0.99335	1.454	300.2	54.77	1.08498	1.626
75.6	36.15	1.02066	1.084	350.3	41.42	1.10559	1.226	50.2	48.56	1.00340	1.460	325.0	55.68	1.09177	1.652
100.6	36.35	1.02976	1.088					75.0	48.91	1.01292	1.468	350.1	56.75	1.09846	1.682
125.5	36.61	1.03852	1.095					100.5	49.33	1.02232	1.479	374.5	57.84	1.10482	1.713
150.5	36.93	1.04696	1.103					125.5	49.74	1.03114	1.489				

$x = 0.05982, \theta = 25.00\text{ }^{\circ}\text{C}$				$x = 0.05982, \theta = 25.00\text{ }^{\circ}\text{C}$				$x = 0.09495, \theta = 25.00\text{ }^{\circ}\text{C}$				$x = 0.09495, \theta = 25.00\text{ }^{\circ}\text{C}$			
p/MPa	t/s	$\rho/\text{g}\cdot\text{cm}^{-3}$	$\eta/\text{mPa}\cdot\text{s}$	p/MPa	t/s	$\rho/\text{g}\cdot\text{cm}^{-3}$	$\eta/\text{mPa}\cdot\text{s}$	p/MPa	t/s	$\rho/\text{g}\cdot\text{cm}^{-3}$	$\eta/\text{mPa}\cdot\text{s}$	p/MPa	t/s	$\rho/\text{g}\cdot\text{cm}^{-3}$	$\eta/\text{mPa}\cdot\text{s}$
0.1	78.7	0.96548	2.380	175.5	103.4	1.01756	3.103	0.1	102.40	0.94511	3.106	125.6	143.04	0.99337	4.307
0.1	78.8	0.96548	2.383	200.4	107.0	1.02363	3.209	0.1	102.87	0.94511	3.120	150.6	151.29	1.00119	4.551
5.6	79.6	0.96743	2.406	225.4	110.5	1.02946	3.310	1.1	102.84	0.94557	3.119	175.5	160.99	1.00861	4.837
10.6	80.2	0.96923	2.425	250.2	114.5	1.03506	3.427	3.0	103.71	0.94645	3.145	200.5	170.03	1.01565	5.104
30.6	83.0	0.97605	2.507	272.2	118.1	1.03987	3.533	5.4	104.31	0.94756	3.162	225.3	179.88	1.02234	5.394
50.1	85.7	0.98243	2.583	297.5	123.1	1.04520	3.679	10.7	106.05	0.94994	3.214	249.8	190.15	1.02864	5.697
75.0	88.9	0.99011	2.678	317.1	126.1	1.04921	3.768	25.4	110.62	0.95640	3.349				
100.6	92.2	0.99763	2.774	337.4	130.6	1.05326	3.900	50.1	118.31	0.96652	3.577				
125.5	95.9	1.00457	2.881	355.2	133.0	1.05673	3.969	75.6	126.37	0.97621	3.815				
150.5	99.7	1.01120	2.993					100.6	134.33	0.98507	4.050				

$x = 0.00982, \theta = 15.00\text{ }^{\circ}\text{C}$				$x = 0.00982, \theta = 15.00\text{ }^{\circ}\text{C}$				$x = 0.02462, \theta = 15.00\text{ }^{\circ}\text{C}$				$x = 0.02462, \theta = 15.00\text{ }^{\circ}\text{C}$			
p/MPa	t/s	$\rho/\text{g}\cdot\text{cm}^{-3}$	$\eta/\text{mPa}\cdot\text{s}$	p/MPa	t/s	$\rho/\text{g}\cdot\text{cm}^{-3}$	$\eta/\text{mPa}\cdot\text{s}$	p/MPa	t/s	$\rho/\text{g}\cdot\text{cm}^{-3}$	$\eta/\text{mPa}\cdot\text{s}$	p/MPa	t/s	$\rho/\text{g}\cdot\text{cm}^{-3}$	$\eta/\text{mPa}\cdot\text{s}$
0.1	47.77	0.99271	1.439	209.8	47.96	1.06849	1.428	0.1	67.36	0.98557	2.031	174.2	67.76	1.04688	2.024
2.8	47.73	0.99388	1.437	232.9	48.48	1.07542	1.442	0.1	67.36	0.98557	2.030	199.0	68.40	1.05440	2.041
5.1	47.58	0.99491	1.432	254.6	49.06	1.08173	1.458	1.4	67.33	0.98609	2.030	222.8	69.05	1.06136	2.059
9.4	47.57	0.99675	1.432	278.1	49.70	1.08838	1.476	3.1	67.17	0.98677	2.025	249.4	69.96	1.06892	2.083
23.9	47.24	1.00289	1.420	301.6	50.43	1.09485	1.496	5.6	67.24	0.98779	2.026	274.8	70.90	1.07590	2.109
47.2	46.89	1.01232	1.408	323.8	51.15	1.10083	1.516	10.5	67.18	0.98979	2.024	299.6	72.03	1.08256	2.141
70.4	46.69	1.02131	1.400					25.5	66.94	0.99571	2.015	324.7	73.12	1.08912	2.171
93.7	46.64	1.02995	1.397					50.3	66.68	1.00514	2.004	348.4	74.30	1.09515	2.204
117.0	46.70	1.03826	1.397					75.5	66.64	1.01432	2.000	371.9	75.69	1.10099	2.243
140.2	46.88	1.04623	1.400					100.5	66.63	1.02304	1.997				
163.5	47.14	1.05392	1.407					125.5	66.92	1.03143	2.004				
186.6	47.51	1.06132	1.416					149.0	67.27	1.03902	2.012				

$x = 0.05982, \theta = 15.00\text{ }^{\circ}\text{C}$				$x = 0.05982, \theta = 15.00\text{ }^{\circ}\text{C}$				$x = 0.05982, \theta = 15.00\text{ }^{\circ}\text{C}$				$x = 0.09495, \theta = 15.00\text{ }^{\circ}\text{C}$			
p/MPa	t/s	$\rho/\text{g}\cdot\text{cm}^{-3}$	$\eta/\text{mPa}\cdot\text{s}$	p/MPa	t/s	$\rho/\text{g}\cdot\text{cm}^{-3}$	$\eta/\text{mPa}\cdot\text{s}$	p/MPa	t/s	$\rho/\text{g}\cdot\text{cm}^{-3}$	$\eta/\text{mPa}\cdot\text{s}$	p/MPa	t/s	$\rho/\text{g}\cdot\text{cm}^{-3}$	$\eta/\text{mPa}\cdot\text{s}$
0.1	124.7	0.97148	3.769	75.6	139.7	0.98352	4.213	221.4	164.4	1.00174	4.947	0.1	166.7	0.95249	5.053
0.1	124.6	0.97148	3.765	100.6	144.0	0.98704	4.342	247.1	168.5	1.00448	5.070	0.1	167.2	0.95249	5.067
5.5	125.9	0.97242	3.802	125.5	148.1	0.99036	4.464	273.4	173.7	1.00716	5.226	25.7	181.8	0.96356	5.501
10.7	127.0	0.97331	3.835	150.5	152.4	0.99353	4.592	298.0	178.3	1.00958	5.363	50.6	196.5	0.97347	5.937
25.7	130.2	0.97583	3.931	174.7	156.3	0.99645	4.707	322.4	182.8	1.01189	5.494	75.6	211.7	0.98273	6.389
50.2	135.0	0.97973	4.075	196.3	159.9	0.99895	4.815	349.8	187.7	1.01439	5.642	100.5	228.1	0.99130	6.874
												125.5	244.9	0.99941	7.371
												150.0	261.9	1.00692	7.874

$x = 0.00982, \theta = 5.00\text{ }^{\circ}\text{C}$				$x = 0.00982, \theta = 5.00\text{ }^{\circ}\text{C}$				$x = 0.02462, \theta = 5.00\text{ }^{\circ}\text{C}$				$x = 0.02462, \theta = 5.00\text{ }^{\circ}\text{C}$			
p/MPa	t/s	$\rho/\text{g}\cdot\text{cm}^{-3}$	$\eta/\text{mPa}\cdot\text{s}$	p/MPa	t/s	$\rho/\text{g}\cdot\text{cm}^{-3}$	$\eta/\text{mPa}\cdot\text{s}$	p/MPa	t/s	$\rho/\text{g}\cdot\text{cm}^{-3}$	$\eta/\text{mPa}\cdot\text{s}$	p/MPa	t/s	$\rho/\text{g}\cdot\text{cm}^{-3}$	$\eta/\text{mPa}\cdot\text{s}$
0.1	66.72	0.99366	2.009	249.4	64.07	1.08698	1.903	0.1	101.41	0.98719	3.057	174.7	94.40	1.05255	2.818
0.1	66.88	0.99366	2.014	274.7	65.00	1.09458	1.929	0.1	100.66	0.98719	3.035	199.7	94.80	1.06056	2.827
3.0	66.61	0.99502	2.006	300.3	65.96	1.10203	1.955	0.1	100.88	0.98719	3.041	224.5	95.46	1.06827	2.844
5.0	66.45	0.99599	2.001	325.3	67.07	1.10908	1.986	0.1	100.47	0.98719	3.029	249.7	96.33	1.07586	2.866
10.4	66.04	0.99851	1.988	348.6	68.19	1.11548	2.017	0.1	100.69	0.98719	3.036	250.4	96.50	1.07604	2.871
25.2	65.05	1.00523	1.956					3.0	100.39	0.98846	3.026	273.5	97.75	1.08281	2.906
50.3	63.70	1.01612	1.912					5.6	100.01	0.98957	3.014	275.1	97.48	1.08327	2.897
75.6	62.81	1.02654	1.883					10.7	99.59	0.99175	3.000	299.2	98.85	1.09014	2.935
100.6	62.34	1.03634	1.866					25.7	98.40	0.99806	2.962	324.5	100.63	1.09716	2.985
125.5	62.10	1.04568	1.856					50.0	96.96	1.00792	2.914	349.0	102.26	1.10377	3.030
150.2	62.19	1.05457	1.856					75.6	95.67	1.01782	2.871	387.8	105.22	1.11394	3.113
174.8	62.34	1.06305	1.858					100.5	94.83	1.02705	2.842				
200.0	62.74	1.07142	1.868					124.3	94.41	1.03552	2.826				
225.0	63.34	1.07942	1.884					149.4	94.29	1.04415	2.819				

Table 3 Continued

$x = 0.05982, \theta = 5.00\text{ }^{\circ}\text{C}$				$x = 0.05982, \theta = 5.00\text{ }^{\circ}\text{C}$				$x = 0.09495, \theta = 5.00\text{ }^{\circ}\text{C}$				$x = 0.09495, \theta = 5.00\text{ }^{\circ}\text{C}$			
p/MPa	t/s	$\rho/\text{g}\cdot\text{cm}^{-3}$	$\eta/\text{mPa}\cdot\text{s}$	p/MPa	t/s	$\rho/\text{g}\cdot\text{cm}^{-3}$	$\eta/\text{mPa}\cdot\text{s}$	p/MPa	t/s	$\rho/\text{g}\cdot\text{cm}^{-3}$	$\eta/\text{mPa}\cdot\text{s}$	p/MPa	t/s	$\rho/\text{g}\cdot\text{cm}^{-3}$	$\eta/\text{mPa}\cdot\text{s}$
0.1	223.6	0.97686	6.754	125.5	255.0	0.99363	7.686	0.1	311.89	0.95989	9.445	44.8	372.04	0.97852	11.24
0.1	223.6	0.97686	6.752	148.0	259.8	0.99624	7.827	0.1	313.00	0.95989	9.478	60.6	394.50	0.98452	11.90
24.1	231.2	0.98041	6.980	174.2	265.3	0.99917	7.990	0.1	312.73	0.95989	9.470	75.6	416.47	0.98996	12.56
50.6	238.6	0.98411	7.198	198.6	270.7	1.00178	8.149	11.1	325.36	0.96474	9.846	90.3	438.76	0.99509	13.22
75.6	244.4	0.98745	7.372	222.9	277.0	1.00430	8.337	15.6	332.17	0.96665	10.05				
100.6	249.8	0.99061	7.532	241.5	280.6	1.00617	8.443	30.6	352.31	0.97287	10.65				
$x = 0.00982, \theta = 0.00\text{ }^{\circ}\text{C}$				$x = 0.00982, \theta = 0.00\text{ }^{\circ}\text{C}$				$x = 0.02462, \theta = 0.00\text{ }^{\circ}\text{C}$				$x = 0.02462, \theta = 0.00\text{ }^{\circ}\text{C}$			
p/MPa	t/s	$\rho/\text{g}\cdot\text{cm}^{-3}$	$\eta/\text{mPa}\cdot\text{s}$	p/MPa	t/s	$\rho/\text{g}\cdot\text{cm}^{-3}$	$\eta/\text{mPa}\cdot\text{s}$	p/MPa	t/s	$\rho/\text{g}\cdot\text{cm}^{-3}$	$\eta/\text{mPa}\cdot\text{s}$	p/MPa	t/s	$\rho/\text{g}\cdot\text{cm}^{-3}$	$\eta/\text{mPa}\cdot\text{s}$
0.1	80.76	0.99358	2.433	174.8	72.70	1.06754	2.166	0.1	127.53	0.98747	3.845	148.9	114.01	1.04423	3.409
0.1	80.92	0.99358	2.438	200.0	73.08	1.07638	2.175	0.3	127.42	0.98757	3.842	174.4	113.83	1.05272	3.399
2.9	80.62	0.99503	2.428	224.3	73.59	1.08463	2.187	1.2	127.21	0.98796	3.835	199.3	114.11	1.06070	3.404
5.2	80.36	0.99616	2.420	249.6	74.31	1.09289	2.206	3.0	126.93	0.98872	3.827	224.4	114.49	1.06854	3.411
10.6	79.65	0.99887	2.398	274.4	75.31	1.10073	2.233	5.5	126.60	0.98983	3.816	249.4	115.49	1.07610	3.437
25.5	78.01	1.00614	2.346	300.3	76.55	1.10863	2.267	10.7	125.60	0.99202	3.784	274.7	116.86	1.08354	3.474
50.5	75.86	1.01779	2.277	325.2	77.69	1.11603	2.298	25.7	123.30	0.99832	3.712	298.1	118.26	1.09022	3.512
75.5	74.35	1.02877	2.228	350.2	78.91	1.12325	2.332	50.6	120.19	1.00838	3.613				
100.6	73.32	1.03922	2.194					74.9	117.60	1.01779	3.530				
125.5	72.84	1.04915	2.176					100.6	115.90	1.02730	3.474				
150.2	72.60	1.05855	2.166					124.0	114.79	1.03565	3.436				
$x = 0.05982, \theta = 0.00\text{ }^{\circ}\text{C}$				$x = 0.05982, \theta = 0.00\text{ }^{\circ}\text{C}$				$x = 0.05982, \theta = 0.00\text{ }^{\circ}\text{C}$				$x = 0.09495, \theta = 0.00\text{ }^{\circ}\text{C}$			
p/MPa	t/s	$\rho/\text{g}\cdot\text{cm}^{-3}$	$\eta/\text{mPa}\cdot\text{s}$	p/MPa	t/s	$\rho/\text{g}\cdot\text{cm}^{-3}$	$\eta/\text{mPa}\cdot\text{s}$	p/MPa	t/s	$\rho/\text{g}\cdot\text{cm}^{-3}$	$\eta/\text{mPa}\cdot\text{s}$	p/MPa	t/s	$\rho/\text{g}\cdot\text{cm}^{-3}$	$\eta/\text{mPa}\cdot\text{s}$
0.1	317.4	0.97921	9.584	50.0	334.0	0.98684	10.08	149.0	356.9	1.00002	10.75	0.10	456.5	0.96362	13.82
0.1	318.2	0.97921	9.608	75.6	340.6	0.99048	10.27	174.3	362.7	1.00305	10.92	12.70	483.8	0.96908	14.63
11.0	322.1	0.98095	9.724	100.6	346.4	0.99386	10.44	196.1	366.9	1.00556	11.04	25.25	511.0	0.97430	15.44
25.6	327.1	0.98321	9.871	125.5	352.0	0.99709	10.61	198.0	368.2	1.00578	11.08	49.77	568.9	0.98393	17.17
$x = 0.00982, \theta = -5.00\text{ }^{\circ}\text{C}$				$x = 0.00982, \theta = -5.00\text{ }^{\circ}\text{C}$				$x = 0.02462, \theta = -5.00\text{ }^{\circ}\text{C}$				$x = 0.02462, \theta = -5.00\text{ }^{\circ}\text{C}$			
p/MPa	t/s	$\rho/\text{g}\cdot\text{cm}^{-3}$	$\eta/\text{mPa}\cdot\text{s}$	p/MPa	t/s	$\rho/\text{g}\cdot\text{cm}^{-3}$	$\eta/\text{mPa}\cdot\text{s}$	p/MPa	t/s	$\rho/\text{g}\cdot\text{cm}^{-3}$	$\eta/\text{mPa}\cdot\text{s}$	p/MPa	t/s	$\rho/\text{g}\cdot\text{cm}^{-3}$	$\eta/\text{mPa}\cdot\text{s}$
0.1	99.8	0.99323	3.007	150.4	85.66	1.06263	2.554	0.1	165.7	0.98750	4.996	149.4	140.4	1.04523	4.198
0.1	100.4	0.99323	3.025	175.3	85.55	1.07224	2.548	5.2	164.4	0.98974	4.955	174.8	139.6	1.05378	4.170
11.5	97.25	0.99940	2.928	200.3	85.92	1.08151	2.555	10.8	162.4	0.99216	4.894	199.9	139.5	1.06197	4.160
26.0	94.66	1.00699	2.847	225.4	86.46	1.09044	2.568	25.6	158.3	0.99845	4.767	225.0	139.8	1.06990	4.166
51.3	91.08	1.01961	2.734	250.4	87.38	1.09900	2.592	30.4	156.9	1.00044	4.722	250.2	140.8	1.07763	4.190
75.6	88.82	1.03099	2.661	275.5	88.18	1.10730	2.612	50.6	152.3	1.00869	4.579	274.6	141.9	1.08491	4.219
76.0	88.84	1.03116	2.662	300.2	89.49	1.11523	2.648	75.0	147.7	1.01827	4.434				
100.6	87.19	1.04209	2.608	325.9	91.33	1.12321	2.699	100.4	144.3	1.02781	4.326				
125.5	86.15	1.05263	2.573	350.9	92.93	1.13074	2.743	124.9	142.0	1.03667	4.250				
$x = 0.05982, \theta = -5.00\text{ }^{\circ}\text{C}$				$x = 0.05982, \theta = -5.00\text{ }^{\circ}\text{C}$				$x = 0.05982, \theta = -10.00\text{ }^{\circ}\text{C}$				$x = 0.05982, \theta = -10.00\text{ }^{\circ}\text{C}$			
p/MPa	t/s	$\rho/\text{g}\cdot\text{cm}^{-3}$	$\eta/\text{mPa}\cdot\text{s}$	p/MPa	t/s	$\rho/\text{g}\cdot\text{cm}^{-3}$	$\eta/\text{mPa}\cdot\text{s}$	p/MPa	t/s	$\rho/\text{g}\cdot\text{cm}^{-3}$	$\eta/\text{mPa}\cdot\text{s}$	p/MPa	t/s	$\rho/\text{g}\cdot\text{cm}^{-3}$	$\eta/\text{mPa}\cdot\text{s}$
0.1	469.8	0.98145	14.18	24.7	481.4	0.99034	14.51	0.1	737.9	0.98351	22.28	125.4	751.9	1.02559	22.56
0.1	471.1	0.98145	14.22	50.3	488.8	0.99921	14.72	30.2	746.2	0.99428	22.49	125.9	753.5	1.02572	22.61
0.1	471.3	0.98145	14.23	75.5	494.0	1.00766	14.86	31.1	746.5	0.99459	22.50	140.9	753.3	1.03034	22.59
0.1	471.5	0.98145	14.23	100.4	498.8	1.01570	14.99	46.4	745.7	0.99987	22.46	146.4	757.8	1.03199	22.71
6.5	474.7	0.98379	14.33	120.6	501.5	1.02205	15.05	79.2	747.2	1.01086	22.47				
11.4	477.6	0.98558	14.41	140.7	505.1	1.02818	15.15	101.0	749.2	1.01790	22.50				

Table 4. Coefficients of Best Fit for Equation 2 (Modified VFT Equation)

x	0 (H ₂ O)	0.00982	0.02462	0.05982	0.09495	0 (D ₂ O)
a	-3.4216	-3.2778	-3.3600	-3.7784	-2.6578	-3.4134
$b\cdot 10^3/\text{MPa}^{-1}$	4.2130	5.0963	5.7191	4.4806	-1.1213	4.8488
$c\cdot 10^6/\text{MPa}^{-2}$	-7.1452	-8.3030	-8.9266	-0.36072	0.0	-8.3586
d/K	479.73	436.59	451.33	499.10	335.70	488.94
$e/(\text{K}\cdot\text{MPa}^{-1})$	-0.66589	-0.70364	-0.68650	-0.29494	0.34141	-0.74755
$f\cdot 10^3/(\text{K}\cdot\text{MPa}^{-2})$	1.5945	1.5386	1.2988	-0.10832	-0.12121	1.7230
$g\cdot 10^7/(\text{K}\cdot\text{MPa}^{-3})$	-7.0780	-6.2832	-2.4950	1.6556	0.0	-6.6113
T_0/K	153.27	168.36	177.23	190.56	209.69	158.72
$\delta (= d/T_0)$	3.13	2.59	2.55	2.62	1.60	3.08
standard uncertainty of fit/%	0.4	0.5	0.4	0.6	0.3	1.4

MPa using spin-echo ¹H NMR.^{16,17} In this temperature range, pure water shows one of its classic “anomalies”; that is, the self-diffusion coefficient initially increases with increasing pressure, passes through a maximum, and then declines.^{15,18–20} Relative to atmospheric pressure values, the maximum is greater in size and shifts slightly to higher pressures, the lower is the temperature. The maximum disappears at approximately 30 °C.

Similar pressure-induced maxima occur for the tracer diffusion of methanol and ethanol at infinite dilution in water, and these are actually larger than for pure water under the same conditions.²¹

These effects are usually interpreted as being due to changes in water structure and the distortion of H-bonding due to an increase in pressure. In nearly all other liquids,

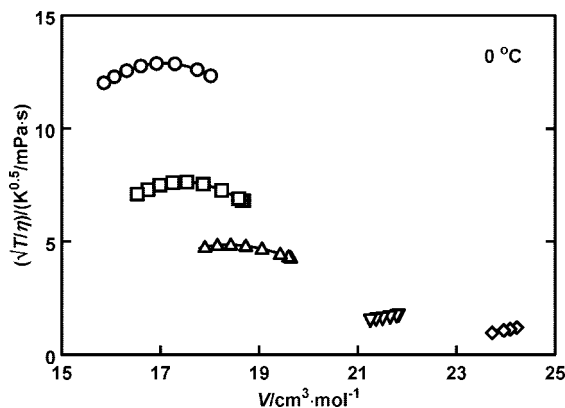


Figure 1. Temperature-corrected fluidity ($\phi = 1/\eta$) of aqueous TBA solutions at 0 °C as a function of molar volume, V . Symbols: \circ , water;³⁷ \square , $x = 0.00982$; \triangle , $x = 0.02462$; ∇ , $x = 0.05982$; \diamond , $x = 0.09495$.

compression slows diffusion. In water, it is supposed that there is a competing effect due to pressure-induced structural change that initially increases molecular mobility. This is stronger at low temperatures, but the effects of compression dominate at higher pressure and at higher temperatures. More subtle interpretations are possible. Errington and Debenedetti,¹⁵ for example, distinguish between a structurally anomalous region where water becomes more disordered when compressed with both translational and orientational order decreasing with increasing density and a region of smaller area (in terms of state points) where the transport property anomalies occur. It should be noted that the pressure dependence of water self-diffusion and viscosity remain unusual above 30 °C, and the self-diffusion coefficient does not show the linear volume dependence typical of (very simple) molecular fluids²² until the temperature is above 100 °C.²³

In dilute water + TBA solutions, the diffusivity-maximum effect is enhanced.^{16,17,24} While the water self-diffusion coefficients are reduced by the presence of the solute as the concentration is increased, as is typical of aqueous nonelectrolyte solutions, the relative self-diffusion coefficients pass through maxima at the lower concentrations and at the lower temperatures. Compared to pure water under the same conditions, the enhancement (relative to atmospheric pressure values) is larger and shifted to higher pressures. That is, the presence of the TBA molecule appears to increase the structure of the water in which it is dissolved. Similar conclusions have been drawn from high-pressure relaxation time studies²⁵ and molecular dynamics simulations.^{26,27}

In our diffusion work, the TBA proton signal was removed by using fully deuterated TBA as the solute. Consequently, there exists the possibility of an isotope effect, though it was argued that this should be small as it was the motion of the water that was being measured, the solutions were dilute, and it was the relative effect of pressure that was being examined at any given composition and temperature. Here we report complementary viscosity measurements on undeuterated water–TBA samples under a similar range of conditions. The results match those of our earlier self-diffusion studies.

Experimental Section

Solutions were prepared from Aldrich TBA, purity 99.5 %, and deionized water (Waters Millipore MilliQ ion-exchange system). Densities at atmospheric pressure were

determined using an Anton-Paar DMA5000 vibrating tube densimeter, with an expanded uncertainty of 0.000 05 g·cm⁻³. The in-built viscosity correction for this instrument has been confirmed for samples with known densities and with viscosities as high as 16 Pa·s.²⁸ TBA mole fractions (x) were calculated from the measured densities using the results of Sakurai for 25 °C.²⁹ The uncertainty in the mole fractions is estimated at $\pm 0.000\ 05$.

The experimental methods for the viscosity measurements have been given previously.^{28,30} In this case, only one sinker was employed, with a nominal diameter of 6.3 mm for which the calibration was determined for 14 measurements with viscosity standard fluids between (0.5 to 202) mPa·s.^{28,30} The fall times are the average of at least three replicates. A combination of the uncertainties in replicate measurements ($\pm 1\ %$) determined from up to ten measurements at randomly selected state points, the calibration ($\pm 1\ %$), and the calibrant viscosities in quadrature yields an expanded uncertainty of $\pm 2\ %$.

Falling body viscosity measurements require an estimate for the density for the buoyancy factor ($1 - \rho/\rho_s$) in the primary working equation

$$\eta(p, T) = \frac{t(1 - \rho/\rho_s)}{A[(1 + 2\alpha(T - T_{\text{ref}})][1 - 2\beta(p - p_{\text{ref}})/3]} \quad (1)$$

where ρ/ρ_s is the ratio of the density ρ for the fluid at the temperature T and pressure p of the measurement to that of the sinker, ρ_s (7.285 g·cm⁻³ at 25 °C). The other quantities in eq 1 are the calibration constant, A [(28.72 \pm 0.03) $\cdot 10^3$ Pa¹], the fall time, t , and α (1.60 $\cdot 10^{-5}$ K⁻¹) and β (2.00 $\cdot 10^{-6}$ MPa⁻¹), the coefficients of expansion and compressibility of the sinker and viscometer tube material, 316 stainless steel, at 25 °C and 0.1 MPa. Solution densities were obtained either from directly measured pVT data,^{31–33} which cover the range $\theta = (5 - 75)$ °C, $p_{\text{max}} = 325$ MPa, $x_{\text{max}} = 0.5$, or by interpolation or extrapolation of Tait equation parameters derived from this data and that for pure water for the temperature and pressure required. Though the Tait parameters are strongly temperature and pressure dependent below $x = 0.2$, the density need only be known to better than 0.5 % to give 0.1 % uncertainty in the buoyancy factor in eq 1. The viscosity tables presented below give sufficient detail for the viscosities to be recalculated should more extensive pVT data become available. The range of pressures covered for each composition and isotherm was limited by the freezing pressures, which vary in a complex way with composition and temperature. There are two eutectic points at atmospheric pressure,³⁴ one at $x = 0.06$ which moves to lower temperatures as the pressure is increased and one at $x = 0.63$ which moves to high temperatures and slightly lower TBA mole fraction as the pressure is increased.^{35,36} It is important to avoid freezing of the samples as then the sample cell usually leaks when the pressure is subsequently released, with consequent contamination of the sample with hydraulic fluid. The isotherm at -10 °C and $x = 0.05982$ was very difficult to measure for this reason as it lies in a narrow liquid “V” between two solid phases (see Figure 4 of ref 17). Replicate data in the tables for $p = 0.1$ MPa reflect repeat fillings and checks that samples had not been contaminated during pressure cycles. A filling can require a resetting of the verticality of the viscometer vessel. The uncertainty for the viscosities includes the effects of such changes: fall-times at a single state point for a given sample have less uncertainty, usually being reproducible within a few tenths of 1 %.

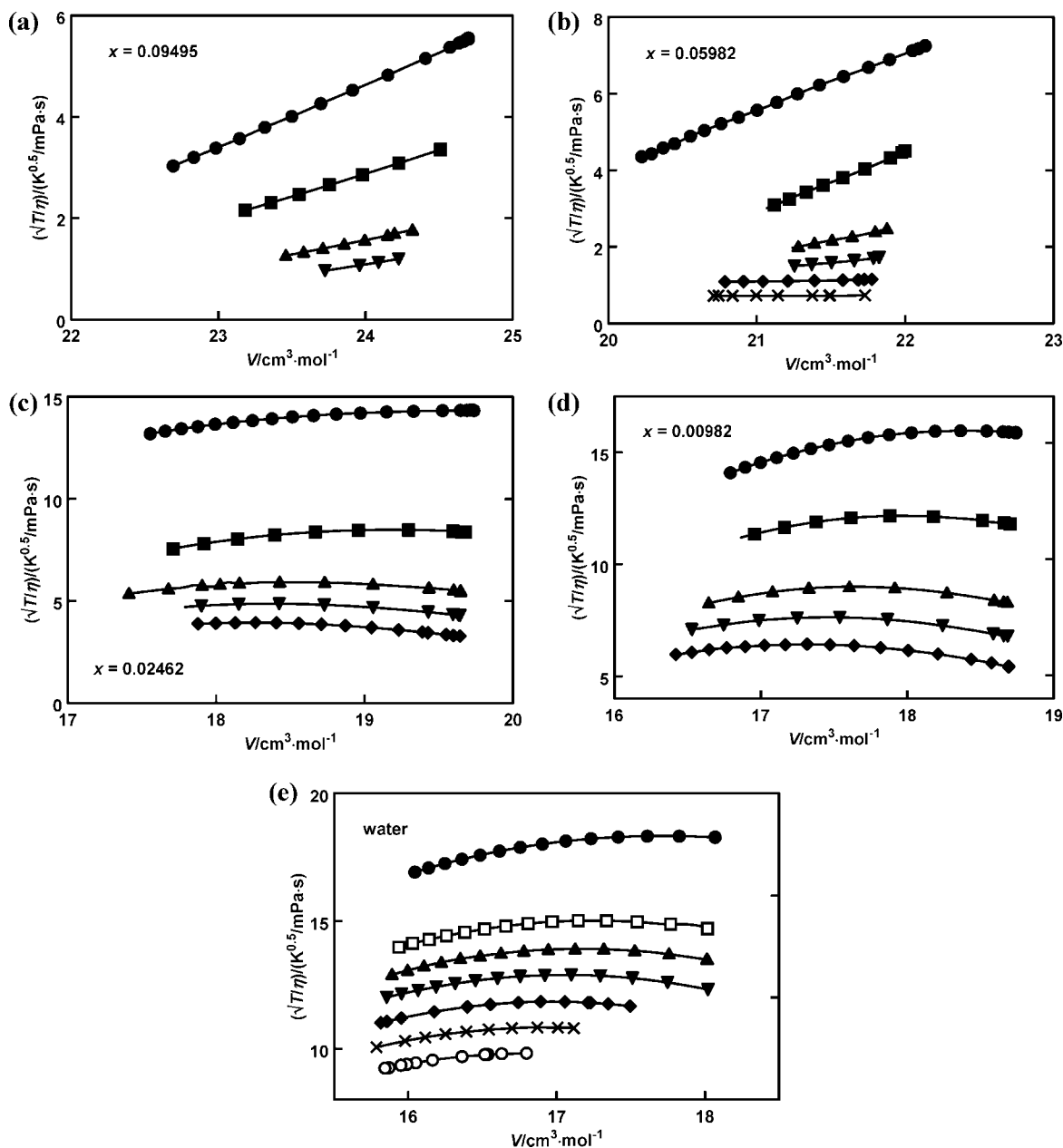


Figure 2. Temperature-corrected fluidity ($\phi = 1/\eta$) of aqueous TBA solutions as a function of molar volume, V . (a) $x = 0.09495$: 25 °C, $(\sqrt{T}/\eta)/(K^{0.5}/\text{mPa}\cdot\text{s}) \equiv y = 1.2575 \cdot (V/\text{cm}^3 \cdot \text{mol}^{-1}) - 25.524$; 15 °C, $y = 0.9087 \cdot (V/\text{cm}^3 \cdot \text{mol}^{-1}) - 18.923$; 5 °C, $y = 0.5868 \cdot (V/\text{cm}^3 \cdot \text{mol}^{-1}) - 12.510$; 0 °C, $y = 0.4653 \cdot (V/\text{cm}^3 \cdot \text{mol}^{-1}) - 10.076$. (b) $x = 0.05982$: 25 °C, $(\sqrt{T}/\eta)/(K^{0.5}/\text{mPa}\cdot\text{s}) \equiv y = 1.5110 \cdot (V/\text{cm}^3 \cdot \text{mol}^{-1}) - 26.183$; 15 °C, $y = 1.5912 \cdot (V/\text{cm}^3 \cdot \text{mol}^{-1}) - 30.521$; 5 °C, $y = 0.7625 \cdot (V/\text{cm}^3 \cdot \text{mol}^{-1}) - 14.226$; 0 °C, $y = 0.3904 \cdot (V/\text{cm}^3 \cdot \text{mol}^{-1}) - 6.8074$. Note that the (-5 and -10) °C isotherms are actually nonlinear. (c) $x = 0.02462$. (d) $x = 0.00982$. (e) Water: data from ref 37. Symbols: ●, 25 °C; ■, 15 °C; □, 10 °C; ▲, 5 °C; ▼, 0 °C; ◆, -5 °C; ×, -10 °C; ○, -15 °C.

Results and Discussion

The density results at atmospheric pressure are presented in Table 1. The Tait equation parameters used at high pressure are given in Table 2.

Table 3 lists the viscosity results. These can be reproduced using a modified Vogel–Fulcher–Tammann equation.

$$\eta/\text{mPa}\cdot\text{s} = \exp\{a + bp + cp^2 + (d + ep + fp^2 + gp^3)/(T - T_0)\} \quad (2)$$

The coefficients are given in Table 4, together with values derived from our earlier measurements for water³⁷ for comparison. (The data are equally well fit if T_0 is allowed to be pressure dependent, as in the equation MVFT2 that we have used elsewhere for ionic liquids.³⁸) The value $T_0 = 153$ K for

water, which can be related to the glass transition temperature T_g ,³⁹ is typical for values derived from bulk transport properties in the liquid region.⁴⁰ It corresponds to $T_g = 160$ K, at the upper end of the range estimated for this substance, for which the glass transition is difficult to characterize.⁴¹ For the TBA solutions, T_0 and the Angell strength parameter ($\delta = d/T_0$) increase and decrease (with some scatter), respectively, with increasing TBA mole fraction. However, given the narrow range of temperatures used in these experiments, these values are best regarded as parameters of best fit, and we do not attempt further interpretation in this paper.

Figures 1 and 2 illustrate the temperature, density, and composition dependence of the viscosity. As the fluidity (reciprocal viscosity, ϕ) for simple molecular fluids, like the

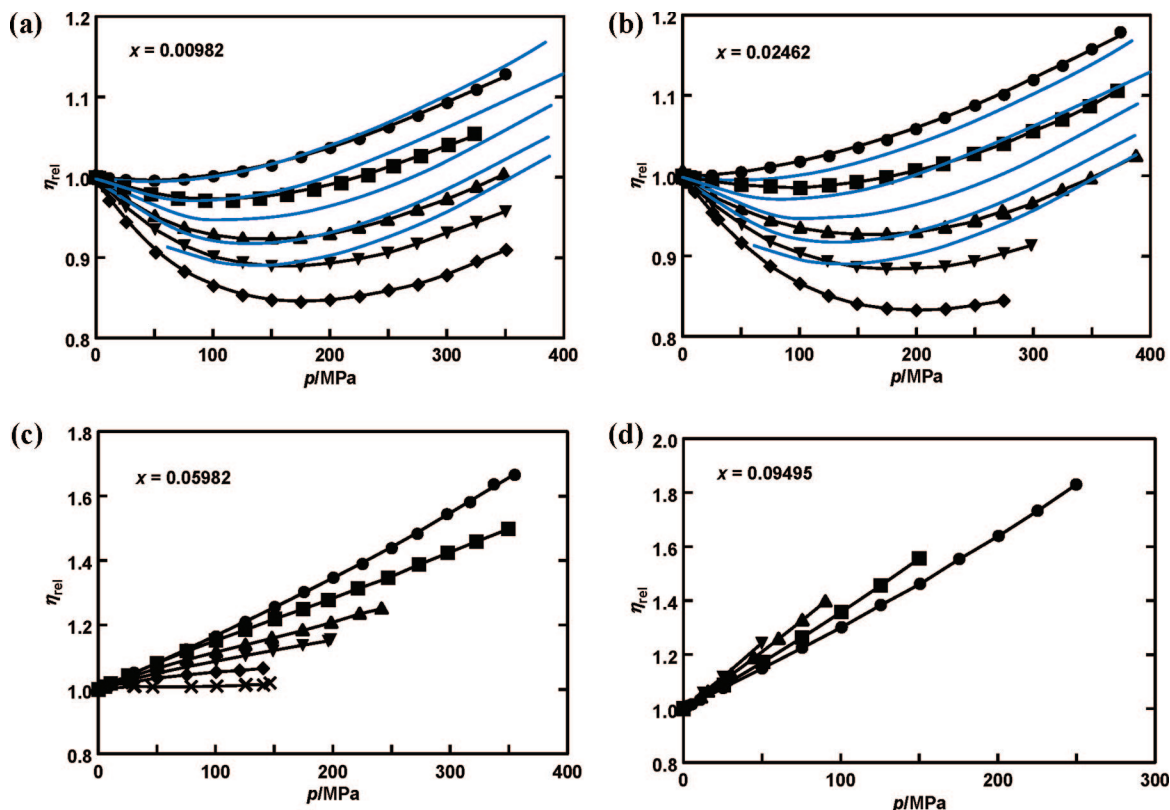


Figure 3. Relative viscosity [$\eta_{\text{rel}} = \eta/\eta(0.1 \text{ MPa})$] of aqueous TBA solutions as a function of pressure, p . The blue curves show η_{rel} for pure water at the same temperatures. Symbols: as in Figure 2. (a) $x = 0.00982$, (b) $x = 0.02462$, (c) $x = 0.05982$, (d) $x = 0.09495$.

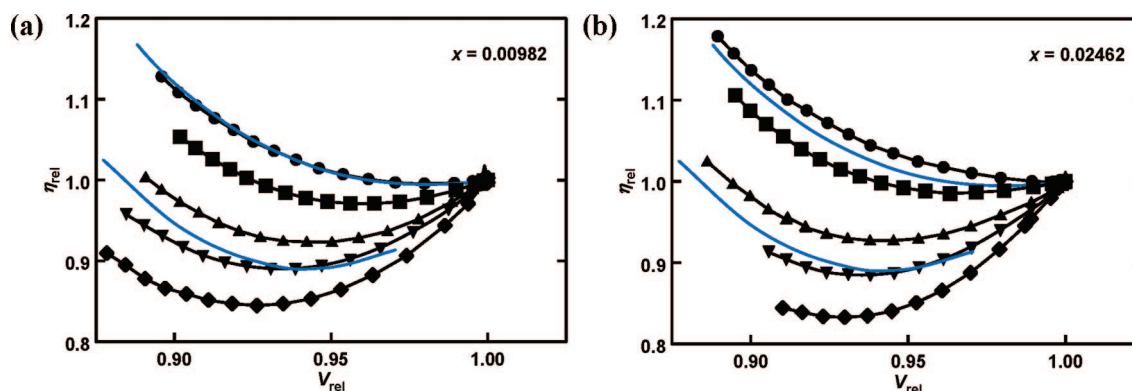


Figure 4. Relative viscosity [$\eta_{\text{rel}} = \eta/\eta(0.1 \text{ MPa})$] of aqueous TBA solutions as a function of relative molar volume, [$V_{\text{rel}} = V/V(0.1 \text{ MPa})$]. The blue curves show η_{rel} for pure water at (25 and -5 °C). Symbols: as in Figure 2. (a) $x = 0.00982$, (b) $x = 0.02462$.

self-diffusion coefficient, is often a simple function of the molar volume, V ,^{30,42,43} the quantity (\sqrt{T}/η) is shown plotted against V in these figures. The \sqrt{T} factor removes the first-order temperature dependence given by simple kinetic theory.²² Figure 1 shows isotherms at 0 °C, illustrating the trends from pure water,³⁷ with its well-established maximum in the fluidity, to mole fraction $x = 0.096$ where the fluidity is a linear function of the molar volume. There is an overall increase in viscosity of an order of magnitude over this range of compositions. Figure 2a shows isotherms for $x = 0.096$: all are linear in V . Figures 2b to 2e show the isotherms for the other compositions, including water. As the solutions become more dilute and the molar volume decreases, the fluidity maxima appear, first at the lower temperatures, then gradually extending to higher temperatures. The positions of the maxima vary with composition and temperature.

The behavior of the fluidity maxima or viscosity minima is made more apparent if relative values are plotted as a function of pressure or volume and compared to those for pure water. Figures 3 and 4 illustrate this. In Figure 4, where the -5 °C isotherm for water is superposed on the plots of the relative viscosity versus the volume ratio, [$k = V(p)/V(0.1 \text{ MPa})$], for $x = 0.01$ and $x = 0.025$, it appears that the effect of the dissolved solute is similar to that of a drop of 5 K in pure water in terms of the effect on the relative viscosity.

The interpretation of these effects is not straightforward without direct structural or spectroscopic studies of water + TBA solutions at the temperatures considered here. Certainly, there are numerous studies at higher temperatures that have concluded that there is hydrophobically driven TBA association in dilute solution. These include NMR relaxation time measurements⁴⁴ where the maximum effect (at 25 °C) was put at $x =$

0.02 to 0.03, consistent with this work and the neutron scattering and computer simulation studies cited in the Introduction.^{7–12,26}

Koga and co-workers,^{45–53} basing their arguments on a large number of thermodynamic property measurements (including heat capacity, expansivity, speed of sound, and particularly their derivatives with respect to composition), have argued that such association occurs at a slightly higher composition, $x = 0.045$. Mizuno and co-workers⁵⁴ have interpreted the composition dependences of water proton and TBA ¹³C NMR chemical shifts and the TBA C–H IR stretching band at 23.3 °C as indicating that there are highly polarized, more strongly H-bonded water molecules in dilute TBA solutions ($x < 0.16$), with the maximum effect at $x = 0.04$.

Of particular interest is the quasi-elastic neutron-scattering study of Calandrini et al.⁵⁵ made at 20 °C. They concluded that the “temperature dependence of the diffusivity parameters in pure water and their concentration dependence in TBA solutions can be rescaled on a common curve attributing to each solution a concentration-dependent “structural temperature” lower than the actual thermodynamic one”. This was reinforced by a subsequent high-pressure study, with measurements made at (–5 and 5) °C.²⁴ There, this relationship was expressed as

$$T_s = T - a'x \quad (3)$$

where T_s is a “structural temperature” and a' had the value (540 ± 40) K. Applying a similar argument to the T_0 values obtained from the VFT fits yields $a' = (534 \pm 62)$ K, which is in good agreement.

Literature Cited

- Apelblat, A. Limiting conductances of electrolytes and the Walden product in mixed solvents in a phenomenological approach. *J. Phys. Chem. B* **2008**, *112*, 7032–7044.
- Stokes, R. H.; Mills, R. *Viscosity of Electrolytes and Related Properties*; Pergamon: Oxford, 1965.
- Broadwater, T. L.; Kay, R. L. Solvent structure in aqueous mixtures. II. Ionic mobilities in *tert*-butyl alcohol - water mixtures at 25°. *J. Phys. Chem.* **1970**, *74*, 3802–3812.
- Barthel, J. M. G.; Krienke, H.; Kunz, W. *Physical Chemistry of Electrolyte Solutions - Modern Aspects*; Springer: Darmstadt, 1998.
- Buck, M. Trifluoroethanol and colleagues: co-solvents come of age. Recent studies with peptides and proteins. *Q. Rev. Biophys.* **1998**, *31*, 297–355.
- Cinelli, S.; Onori, G.; Santucci, A. Effect of 1-alcohols on micelle formation and protein folding. *Colloids Surf. A* **1999**, *160*, 3–8.
- Finney, J. L.; Bowron, D. T.; Daniel, R. M.; Timmins, P. A.; Roberts, M. A. Molecular and mesoscale structures in hydrophobically driven aqueous solutions. *Biophys. Chem.* **2003**, *105*, 391–409.
- Bowron, D. T.; Finney, J. L.; Soper, A. K. Structural investigation of solute-solute interactions in solutions of tertiary butanol. *J. Phys. Chem. B* **1998**, *102*, 3551–3563.
- Finney, J. L.; Bowron, D. T.; Soper, A. K. The structure of aqueous solutions of tertiary butanol. *J. Phys.: Condens. Matter* **2000**, *12*, A123–A128.
- Bowron, D. T.; Soper, A. K.; Finney, J. L. Temperature dependence of the structure of a 0.06 mole fraction tertiary butanol-water solution. *J. Chem. Phys.* **2001**, *114*, 6203–6219.
- Bowron, D. T. Structure and interactions in simple solutions. *Philos. Trans. R. Soc. London B* **2004**, *359*, 1167–1180.
- Bowron, D. T.; Finney, J. L. Association and dissociation of an aqueous amphiphile at elevated temperatures. *J. Phys. Chem. B* **2007**, *111*, 9838–9852.
- Ben-Naim, A. Y. *Hydrophobic Interactions*; Springer: Berlin, 1980.
- Southall, N. T.; Dill, K. A.; Haymet, A. D. J. A view of the hydrophobic effect. *J. Phys. Chem. B* **2002**, *106*, 521–533.
- Errington, J. R.; Debenedetti, P. G. Relationship between structural order and the anomalies of liquid water. *Nature* **2001**, *409*, 318–321.
- Harris, K. R.; Newitt, P. J. Diffusion and Structure in water-alcohol mixtures: evidence for the effects of large apolar solutes on water. *J. Phys. Chem. B* **1998**, *102*, 8874–8879.
- Harris, K. R.; Newitt, P. J. Diffusion and structure in water-alcohol mixtures: water + *tert*-butanol (2-methyl-2-propanol). *J. Phys. Chem. A* **1999**, *103*, 6508–6513.
- Woolf, L. A. Tracer diffusion of tritiated-water (THO) in ordinary water (H₂O) under pressure. *J. Chem. Soc., Faraday Trans. I* **1975**, *71*, 784–796.
- Harris, K. R.; Woolf, L. A. The pressure and temperature dependence of the selfdiffusion coefficient of ordinary water and oxygen-18 water. *J. Chem. Soc., Faraday Trans. I* **1980**, *76*, 377–385.
- Harris, K. R.; Newitt, P. J. The self-diffusion coefficient of water at low temperatures and high pressure. *J. Chem. Eng. Data* **1997**, *42*, 346–349.
- Easteal, A. J.; Woolf, L. A. Pressure and temperature dependence of tracer diffusion coefficients of methanol, ethanol, acetonitrile, and formamide in water. *J. Phys. Chem.* **1985**, *89*, 1066–1069.
- Van Loef, J. J. The corrected Enskog theory and the transport properties of molecular liquids. *Physica* **1977**, *87A*, 258–272.
- Wilbur, D. J.; DeFries, T.; Jonas, J. Self-diffusion in compressed liquid heavy water. *J. Chem. Phys.* **1976**, *65*, 1783–1786.
- Calandrini, V.; Deriu, A.; Onori, G.; Paciaroni, A.; Telling, M. T. F. Pressure effect on water dynamics in *tert*-butyl alcohol/water solutions. *J. Phys.: Condens. Matter* **2006**, *18*, S2363–S2371.
- Yoshida, K.; Ibuki, K.; Ueno, M. Pressure and temperature effects on ²H spin-lattice relaxation times and ¹H chemical shifts in *tert*-butyl alcohol and urea-D₂O solutions. *J. Chem. Phys.* **1998**, *104*, 1360–1367.
- Tanaka, H.; Nakanishi, K.; Touhara, H. Computer experiments on aqueous solutions. VI. Potential energy function for *tert*-butyl alcohol dimer and molecular dynamics calculation of 3 mol% aqueous solution of *tert*-butyl alcohol. *J. Chem. Phys.* **1984**, *81*, 4065–4073.
- Kusalik, P. G.; Lyubartsev, A. P.; Bergman, D. L.; Laaksonen, A. Computer simulation of *tert*-butyl alcohol. 2. Structure in aqueous solution. *J. Phys. Chem. B* **2000**, *104*, 9533–9539.
- Harris, K. R.; Kanakubo, M.; Woolf, L. A. Temperature and pressure dependence of the viscosity of the ionic liquid 1-methyl-3-octylimidazolium hexafluorophosphate and 1-methyl-3-octylimidazolium tetrafluoroborate. *J. Chem. Eng. Data* **2006**, *51*, 1161–1167.
- Sakurai, M. Partial molar volumes in aqueous mixtures of non-electrolytes. I. *t*-Butyl alcohol. *Bull. Chem. Soc. Jpn.* **1987**, *60*, 1–7.
- Harris, K. R. Temperature and density dependence of the viscosity of toluene. *J. Chem. Eng. Data* **2000**, *45*, 893–897.
- Nakagawa, M.; Inubushi, H.; Moriyoshi, T. Compressions of water + *t*-butanol mixtures at 298.15 K and pressures up to 142 MPa. *J. Chem. Thermodyn.* **1981**, *13*, 171–178.
- Kubota, H.; Tanaka, Y.; Makita, T. Volumetric behavior of pure alcohols and their water mixtures under high pressure. *Int. J. Thermophys.* **1987**, *8*, 47–70.
- Harris, K. R.; Newitt, P. J.; Back, P. J.; Woolf, L. A. Thermodynamic property measurements for 2-methylpropan-2-ol + water from the freezing surface to 75 °C. *High Temp. High Pressures* **1998**, *30*, 51–62.
- Ott, J. B.; Goates, J. R.; Waite, B. A. (Solid + liquid) phase equilibria and solid-hydrate formation in water + methyl, + ethyl, + isopropyl, and + tertiary butyl alcohols. *J. Chem. Thermodyn.* **1979**, *11*, 739–746.
- Woznyj, M. Hochdruck-kernresonanzuntersuchungen zur molekularen Dynamik und Struktur des binären Systems *t*-Butanol/D₂O. Thesis, Universität Regensburg, Germany, 1985.
- Woznyj, M.; Lüdemann, H.-D. The pressure dependence of the phase-diagram of *t*-butanol-water. *Z. Naturforsch. A* **1985**, *40*, 693–698.
- Harris, K. R.; Woolf, L. A. Temperature and volume dependence of the viscosity of water and heavy water at low temperatures. *J. Chem. Eng. Data* **2004**, *49*, 1064–1069; 1851.
- Harris, K. R.; Kanakubo, M.; Woolf, L. A. Temperature and pressure dependence of the viscosity of the ionic liquids 1-hexyl-3-methylimidazolium hexafluorophosphate and 1-butyl-3-methylimidazolium bis-(trifluorosulfonyl) imide. *J. Chem. Eng. Data* **2006**, *52*, 1080–1085.
- Angell, C. A. Liquid fragility and the glass transition in water and aqueous solutions. *Chem. Rev.* **2002**, *102*, 2627–2650.
- Price, W. S.; Ide, H.; Arata, Y. Self-diffusion of supercooled water to 238 K using PGSE NMR diffusion measurements. *J. Phys. Chem. A* **1999**, *103*, 448–450.
- Angell, C. A. Insights into phases of liquid water from study of its unusual glass-forming properties. *Science* **2008**, *319*, 582–587.
- Van Loef, J. J. Atomic and electronic transport properties and the molar volume of monatomic liquids. *Physica* **1974**, *75*, 115–132.
- Harris, K. R. Temperature and density dependence of the selfdiffusion coefficient of *n*-hexane from 223 to 333 K and up to 400 MPa. *J. Chem. Soc., Faraday Trans. I* **1982**, *78*, 2265–2275.
- Mayele, M.; Holz, M.; Sacco, A. NMR studies on hydrophobic interactions in solution. Part 4. Temperature and concentration dependence of the hydrophobic self-association of *tert*-butanol in water. *Phys. Chem. Chem. Phys.* **1999**, *1*, 4615–4618.
- Koga, Y. An SAXS study of concentration fluctuations in *tert*-butanol water-system. *Chem. Phys. Lett.* **1984**, *111*, 176–180.

- (46) Koga, Y. Excess partial molar enthalpies of tert-butanol in water tert-butanol mixtures. *Can. J. Chem.* **1988**, *66*, 1187–1193.
- (47) Koga, Y. Excess partial molar enthalpies of water in water-tert-butanol mixtures. *Can. J. Chem.* **1988**, *66*, 3171–3175.
- (48) Koga, Y.; Wong, T. Y. H.; Siu, W. W. Y. Vapor-pressure of aqueous tert-butanol in the water-rich region - transition in the mixing scheme. *Thermochim. Acta* **1990**, *169*, 27–38.
- (49) Koga, Y. Vapor-pressures of dilute aqueous t-butyl alcohol - how dilute is the Henry's law region. *J. Phys. Chem.* **1995**, *99*, 6231–6233.
- (50) Koga, Y. Mixing schemes in aqueous solutions of nonelectrolytes: a thermodynamic approach. *J. Phys. Chem.* **1996**, *100*, 5172–5181.
- (51) Tamura, K.; Osaki, A.; Koga, Y. Compressibilities of aqueous tert-butanol in the water-rich region at 25 degrees C: partial molar fluctuations and mixing schemes. *Phys. Chem. Chem. Phys.* **1999**, *1*, 121–126.
- (52) Koga, Y.; Nishikawa, K.; Westh, P. "Icebergs" or no "Icebergs" in aqueous alcohols?: composition-dependent mixing schemes. *J. Phys. Chem. A* **2004**, *108*, 3873–3877.
- (53) Perera, A.; Sokolić, F.; Almásy, L.; Koga, Y. Kirkwood-Buff integrals of aqueous alcohol binary mixtures. *J. Chem. Phys.* **2006**, 124515-1–124515-9.
- (54) Mizuno, K.; Kimura, Y.; Morichika, H.; Nishimura, Y.; Shimada, S.; Maeda, S.; Imafuji, S.; Ochi, T. Hydrophobic hydration of tert-butyl alcohol probed by NMR and IR. *J. Mol. Liq.* **2000**, *85*, 139–152.
- (55) Calandrini, V.; Deriu, A.; Onori, G.; Lechner, R. E.; Pieper, J. Diffusive dynamics of water in tert-butyl alcohol/water mixtures. *J. Chem. Phys.* **2004**, *120*, 4759–4767.

Received for review July 1, 2008. Accepted August 13, 2008.

JE800504N